

Finite Volume Schemes for Solving Nonlinear Partial Differential Equations in Financial Mathematics

Pavol Kútik and Karol Mikula

Abstract In order to estimate a fair value of financial derivatives, various generalizations of the classical linear Black-Scholes parabolic equation have been made by adjusting the constant volatility to be a function of the option price itself. We present a second order numerical scheme, based on the finite volume method discretization, for solving the so-called Gamma equation of the Risk Adjusted Pricing Methodology (RAPM) model. Our new approach is based on combination of the fully implicit and explicit schemes where we solve the system of nonlinear equations by iterative application of the semi-implicit approach. Presented numerical experiments show its second order accuracy for the RAPM model as well as for the test with exact Barenblatt solution of the porous-medium equation which has a similar character as the Gamma equation.

1 Motivation from Financial Mathematics

Black-Scholes linear model. Modeling financial derivative prices by PDEs has been introduced in 1973, when a simple linear model was derived by Black and Scholes [4] and independently by Merton [10]. Its simplicity is obtained by imposing a couple of limiting assumptions [8] which in reality do not always hold. Nevertheless, it is still considered as the cornerstone when deriving more general ones. To obtain the governing PDE, Black and Scholes assumed that the underlying asset S follows a geometric Brownian motion $dS = (\mu - q)Sdt + \hat{\sigma}SdW$, where $\mu > 0$ is a constant drift, $\hat{\sigma} > 0$ is a constant volatility parameter of the underlying asset, q is a constant asset dividend yield rate and W is a standard Wiener process. Denoting the price of an option as $V(S, t)$ and applying Itô's lemma to obtain the stochastic differential dV , they derived a parabolic partial differential equation for valuation of options [14]:

$$\frac{\partial V}{\partial t} + \frac{\hat{\sigma}^2}{2} S^2 \frac{\partial^2 V}{\partial S^2} + (r - q)S \frac{\partial V}{\partial S} - rV = 0, \quad (1)$$

where r represents the riskless interest rate. To complete the formulation of the option pricing model, we need to prescribe a terminal pay-off condition at expiration time T . In the case of an European call option the terminal pay-off condition is

Pavol Kútik, Karol Mikula
Department of Mathematics, Radlinského 11, 813 68, Bratislava, Slovak University of Technology,
e-mail: kutik@math.sk, mikula@math.sk

$$V(S, T) = \max(S - E, 0), \quad (2)$$

where E denotes the strike price. For plain vanilla options, like the simple call or simple put option, an exact solution to (1)-(2) is known [14].

Nonlinear extensions. Note that in equation (1) the volatility is constant. However, if we insert real data into the model and compute inversely the implied volatility, it is not constant [8]. More generally, the volatility parameter can be defined by $\sigma = \sigma(\partial_S^2 V, S, T - t)$, where $\partial_S^2 V$ is the so-called Γ of an option. In financial theory and practice various nonlinear generalizations of Black-Scholes linear model exist with such defined volatility function. For instance, Leland in [9] proposed a model which takes transaction costs into account. In order to describe option pricing in incomplete markets Avellaneda, Levy and Paras in [1] used a jumping volatility function. Barles and Soner in their model [3] adjusted the volatility depending on investor's preferences. Illiquid market effects due to large traders choosing given stock-trading strategies were studied by Frey in [5] and by Schönbucher and Wilmott in [12]. A further interesting nonlinear model which we deal with in this paper is the so-called **Risk Adjusted Pricing Methodology (RAPM) model** derived by Kratka in [7] and further generalized by Jandačka and Ševčovič in [6]. Notice that the numerical scheme presented in the next section can be applied to all the above mentioned models since they can be represented by a PDE in the general form (6). Interestingly, the nonlinear porous-medium equation (14) which we deal with in the last section is also a special case of the Gamma equation (6).

The RAPM model omits the limiting assumption of having no transaction costs. Hence, it assumes that the portfolio is hedged only at discrete times, since continuous rehedgeing would lead to infinite transaction costs. The more often the portfolio is being rehedgeing, the higher the risk associated with transaction costs become. On the other hand, seldom rehedgeing implies higher risk arising from its weak protection against the movement of the underlying assets's price. Hence, there exists an optimal time step, representing the hedge interval, for which the sum of both risks is minimal. Using such ideas, the governing PDE for the RAPM model in the following form is obtained [6]:

$$\frac{\partial V}{\partial t} + \frac{1}{2} \hat{\sigma}^2 S^2 \left[1 + \mu \left(S \frac{\partial^2 V}{\partial S^2} \right)^{\frac{1}{3}} \right] \frac{\partial^2 V}{\partial S^2} + (r - q) S \frac{\partial V}{\partial S} - rV = 0, \quad (3)$$

where $\mu = 3 \left(\frac{C^2 R}{2\pi} \right)^{\frac{1}{3}}$, $C \geq 0$ represents the relative transaction costs for buying or selling on stock and $R \geq 0$ is the marginal value of investor's exposure to risk. Note that the diffusion coefficient in (3) is dependent on Γ , thus the equation is a nonlinear PDE. Since $1 + \mu (S\Gamma)^{\frac{1}{3}} \geq 1$, the option price computed by this equation is slightly above that from the linear Black-Scholes model, i.e. we obtain a so-called Ask price. If the diffusion coefficient is of the form $1 - \mu (S\Gamma)^{\frac{1}{3}} \leq 1$, then we get the lower Bid price of an option. Let us note that we can rewrite the equation (3) as

$$\frac{\partial V}{\partial t} + S\beta(S\Gamma) + (r-q)S\frac{\partial V}{\partial S} - rV = 0, \quad (4)$$

where $\beta(H) = \frac{1}{2}\sigma^2 \left(1 + \mu H^{\frac{1}{3}}\right)H$. Since the equation (4) contains the term $S\Gamma$ it is convenient to introduce the following transformation:

$$H(x, \tau) = S\Gamma = S\partial_S^2 V(S, t), \quad (5)$$

where the new variables, x and τ , are obtained by transforming the original ones using the standard substitution: $x = \ln\left(\frac{S}{E}\right)$, $x \in \mathbb{R}$ and $\tau = T - t$, $\tau \in (0, T)$. If we take the second derivative of equation (4) with respect to x it turns out that the function $H(x, \tau)$ is a solution to the following nonlinear parabolic differential equation, the so-called **Gamma equation** [13]:

$$\frac{\partial H(x, \tau)}{\partial \tau} = \frac{\partial^2 \beta(H)}{\partial x^2} + \frac{\partial \beta(H)}{\partial x} + (r-q)\frac{\partial H(x, \tau)}{\partial x} - qH(x, \tau). \quad (6)$$

Notice that unlike in equation (3), all terms containing spatial derivatives in the Gamma equation (6) are in divergent form, thus it is suitable to use finite volume method discretization which follows. Concerning the boundary conditions, since the second derivative of $V(S, t)$ with respect to S tends asymptotically to zero as $S \rightarrow 0$, respectively $S \rightarrow \infty$, from (5) it follows that the transformed Dirichlet boundary conditions are $H(-\infty, \tau) = H(\infty, \tau) = 0$.

2 Finite Volume Approximation Schemes

The most general form of the Gamma equation is as follows:

$$\frac{\partial H(x, \tau)}{\partial \tau} = \frac{\partial^2 \beta(H, x, \tau)}{\partial x^2} + \frac{\partial \beta(H, x, \tau)}{\partial x} + f(x)\frac{\partial H(x, \tau)}{\partial x} + g(x)H(x, \tau), \quad (7)$$

Notice that

$$\frac{\partial^2 \beta(H(x, \tau), x, \tau)}{\partial x^2} = \frac{\partial}{\partial x} \left(\beta'_H(H, x, \tau)\frac{\partial H(x, \tau)}{\partial x} + \beta'_x(H, x, \tau) \right), \quad (8)$$

where $\beta'_H(H, x, \tau)$ and $\beta'_x(H, x, \tau)$ are partial derivatives of the function $\beta(H(x, \tau), x, \tau)$ by H and x , respectively. Moreover,

$$f(x)\frac{\partial H(x, \tau)}{\partial x} = \frac{\partial}{\partial x} (f(x)H(x, \tau)) - H(x, \tau)f'_x(x). \quad (9)$$

Inserting (8) and (9) into (7) and integrating over the finite volume $(x_{i-\frac{1}{2}}, x_{i+\frac{1}{2}})$, with center point denoted by x_i , we get

$$\begin{aligned} \int_{x_{i-\frac{1}{2}}}^{x_{i+\frac{1}{2}}} \frac{\partial H}{\partial \tau} dx &= \int_{x_{i-\frac{1}{2}}}^{x_{i+\frac{1}{2}}} \frac{\partial}{\partial x} \left(\beta'_H \frac{\partial H}{\partial x} + \beta'_x + \beta + f(x)H \right) dx \\ &+ \int_{x_{i-\frac{1}{2}}}^{x_{i+\frac{1}{2}}} (g(x) - f'_x(x)) H dx. \end{aligned} \quad (10)$$

Using central spatial differences, Newton-Leibniz formula, the mid-point rule and notations

$$\beta_{i+\frac{1}{2}}^* = \beta(H_{i+\frac{1}{2}}^*, x_{i+\frac{1}{2}}, \tau_*) , \beta'_{x_{i+\frac{1}{2}}} = \beta'_x(H_{i+\frac{1}{2}}^*, x_{i+\frac{1}{2}}, \tau_*) , \beta'_{H_{i+\frac{1}{2}}} = \beta'_H(H_{i+\frac{1}{2}}^*, x_{i+\frac{1}{2}}, \tau_*) ,$$

we obtain the following *general numerical scheme* for solving (7):

$$\begin{aligned} h \frac{H_i^{j+1} - H_i^j}{k} &= \beta'_{H_{i+\frac{1}{2}}}^* \frac{H_{i+\frac{1}{2}}^* - H_i^*}{h} - \beta'_{H_{i-\frac{1}{2}}}^* \frac{H_i^* - H_{i-\frac{1}{2}}^*}{h} + \beta'_{x_{i+\frac{1}{2}}}^* - \beta'_{x_{i-\frac{1}{2}}}^* + \beta_{i+\frac{1}{2}}^* \\ &- \beta_{i-\frac{1}{2}}^* + f(x_{i+\frac{1}{2}}) \frac{H_{i+\frac{1}{2}}^* + H_i^*}{2} - f(x_{i-\frac{1}{2}}) \frac{H_i^* + H_{i-\frac{1}{2}}^*}{2} + h H_i^* (g(x_i) - f'_x(x_i)), \end{aligned} \quad (11)$$

where H_i^j represents the approximate value of the solution in point x_i at time τ_j and $\star \in \{j, j+1\}$ represents the chosen time layer. Depending on in which time we evaluate the terms on the right-hand side in (11) we obtain three distinct first-order schemes.

Explicit scheme is obtained by taking all terms from the old time layer, i.e. $\star = j$.

Semi-implicit scheme is obtained by taking all linear terms from the old time layer, i.e. $\star = j$, and all nonlinear terms from the new time layer, i.e. $\star = j+1$. The solution is found by solving a tridiagonal system of linear equations by the Thomas algorithm.

Fully-implicit scheme is obtained if all terms are taken from the new time layer, i.e. $\star = j+1$. We get a system of nonlinear equations. The algorithm for solving such a system is based on iterative solution of the semi-implicit scheme. We start the iterative process by assigning the old time step solution vector to the starting iteration solution vector for the new time step. Then, in each iteration, we insert the solution vector into the nonlinear terms, to get their actual iteration. If we collect all unknowns from the solution vector, i.e. the linear terms from the new layer, on the left-hand side and all remaining terms, i.e. the nonlinear terms and the linear term from the old layer, on the right-hand side we obtain a linear tridiagonal system for determining next iteration of the solution vector. The whole process is terminated when the successive solution vectors are close enough [2].

New second order scheme is of the **Crank-Nicolson type** and is obtained by the arithmetic average of the explicit and the fully-implicit scheme. The system of nonlinear equations has a similar structure to that from the fully-implicit scheme, thus we solve it using the same principles.

As noticed above, the linear systems arising in our schemes are solved by the Thomas algorithm. Its numerical stability is guaranteed by the strict diagonal dom-

inance of the system matrix which can be always achieved by a suitable choice of time step k in (11). Another important issue is the study of stability which is usually related to the approximation of diffusion and advection terms. Inspecting the Gamma equation (6), one can see that the diffusion coefficient is given by β'_H while the speed of the advection is proportional to $\beta'_H + r - q$ and thus in the studied application they are comparable ($\hat{\sigma}^2 \approx r - q$). The fully explicit scheme gives oscillations for the coupling $k \approx h$ due to violating the CFL condition in approximation of the diffusion term. On the other hand, all other schemes are implicit and we did not observe any oscillations, mainly due to the fact that the advection does not dominate the diffusion.

3 Numerical Experiments

Three different numerical experiments were made. The first two are concerned with the approximate solution to the RAPM Gamma equation and the last one deals with the numerical solution to a nonlinear porous-medium PDE.

RAPM Gamma equation experiments. As no comparative exact solution to such an equation is known, a natural choice is to take the exact solution of the linear Black-Scholes model. Clearly, to maintain the equality in the Gamma equation we have to add a residual term $Res(x, \tau)$ into (6) which balances the difference between the Black-Scholes solution and the higher Ask price of the RAPM model:

$$\frac{\partial H}{\partial \tau} = \frac{\partial^2 \beta}{\partial x^2} + \frac{\partial \beta}{\partial x} + (r - q) \frac{\partial H}{\partial x} - qH + Res, \quad (12)$$

where $\beta(H) = \frac{\hat{\sigma}^2}{2} (1 + \mu H^{\frac{1}{3}})H$. The first two experiments differ from each other in two main aspects: the coefficient μ and the initial condition. Following parameters were set for both cases the same: $\hat{\sigma} = 0.30$, $r = 0.03$, $q = 0.01$, $E = 25$. In all numerical experiments we impose boundary conditions $H(x_L, \tau) = H(x_R, \tau) = 0$, where x_L and x_R are boundaries of the space interval.

The intention of *the first experiment* is to show how well the proposed numerical schemes can handle the nonlinearity in the Gamma equation (12). We put the coefficient $\mu = 0.2$, hence the function $\beta(H)$ is nonlinear. As the initial condition $H(x, \tau_0)$ we consider Black-Scholes solution $V(S, T - \tau_0)$ transformed by (5), in time $\tau_0 = 1$. Measurements of the estimated error $\|e_n^m\|_{L_2}$ are done by comparison with the exact solution $H(x, \tau)$ to (12) for $\tau > \tau_0$. Since all first-order schemes exhibited very similar features, we show here outputs just for the semi-implicit scheme. The reason for exclusion of the explicit scheme was its instability using coupling $k = h$. Regarding the fully-implicit scheme, experiments show that the accuracy of the semi-implicit scheme is very close to the fully-implicit scheme, thus it is sufficient to use just the former one which is less time consuming. The experiment was done on the time-space domain $(x, \tau) = [-2, 2] \times [1, 2]$. Tables 1 and 2 indicate that for this type of problem the semi-implicit scheme is first order accurate while the Crank-Nicolson type scheme is second order accurate.

Table 1 Outputs obtained by solving the RAPM Gamma equation (12) ($\tau_0 = 1, k = h$) using the semi-implicit scheme: estimated error $\|e_n^m\|_{L_2}$, CPU-time and EOC with respect to $\|e_n^m\|_{L_2}$.

n	h	$\ e_n^m\ _{L_2}$	CPU	$EOC_{k \sim h}$
20	0.1	0.00777657	2.231	-
40	0.05	0.00333385	9.126	1.22194
80	0.025	0.00153036	36.614	1.12332
160	0.0125	0.00073141	147.078	1.06512
320	0.00625	0.00035733	582.929	1.03343

Table 2 Outputs obtained by solving the RAPM Gamma equation (12) ($\tau_0 = 1, k = h$) using the Crank-Nicolson type scheme: estimated error $\|e_n^m\|_{L_2}$, CPU-time and EOC with respect to $\|e_n^m\|_{L_2}$.

n	h	$\ e_n^m\ _{L_2}$	CPU	$EOC_{k \sim h}$
20	0.1	0.00272286	4.383	-
40	0.05	0.000666762	17.785	2.02988
80	0.025	0.000165182	71.136	2.01311
160	0.0125	0.0000412598	294.062	2.00125
320	0.00625	0.0000108204	1206.53	1.93099

In the *the second experiment* we set $\mu = 0$ and we show how the regularization of the transformed initial condition and the backward transformation of the Gamma equation solution affects the total accuracy of the method. In this case the solution of the Gamma equation coincides with the transformed solution $H(x, \tau)$ of the linear Black-Scholes equation (1) which implies that the residual term in (12) is zero. The initial condition $H(x, \tau_0)$ is considered for $\tau_0 = 0$. Hence the transformed payoff function, see (2) and (5), is the Dirac delta function, $H(x, 0) = \delta(x)$, $x \in \mathbb{R}$. In order to get a suitable initial condition for our computation, we consider its regularization given by the function $H(x, 0) = \frac{N'(d)}{\hat{\sigma}\sqrt{\tau^*}}$, where $\tau^* > 0$ is sufficiently small, $N(d)$ is the cumulative distribution function of the normal distribution and $d = \frac{x+(r-q-\hat{\sigma}^2/2)\tau^*}{\hat{\sigma}\sqrt{\tau^*}}$ [13]. The backward transformation of numerical solution is done by using formula

$$\begin{aligned}
V(S_k, T - \tau_j) &= h \sum_{i=-n}^n \max(S_k - Ee^{x_i}, 0) H_i^j = h \sum_{i=-n}^k (S_k - Ee^{x_i}) H_i^j \\
&= h S_k \sum_{i=-n}^k H_i^j - h E \sum_{i=-n}^k e^{x_i} H_i^j = h S_k F_k - h E G_k, \quad (13)
\end{aligned}$$

where $F_k = F_{k-1} + H_k^j$, $G_k = G_{k-1} + e^{x_k} H_k^j$ and $S_k = Ee^{x_k}$. Formula (13) is obtained by integration of (5). Measurements of the estimated error $\|e_n^m\|_{L_2}$ are done by comparison with the Black-Scholes solution $V(S, t)$. However, in practice, doing computations with such an initial condition is not as straightforward task as in the first experiment. The problem is that we do not know a priori the optimal value of τ^* for a given time-space mesh. We consider the optimal value of τ^* as a value for which the estimated error of the numerical solution is minimized. Numerical outputs for the discretized time-space domain $(x, \tau) = [-2, 2] \times [0, 1]$ are summarized

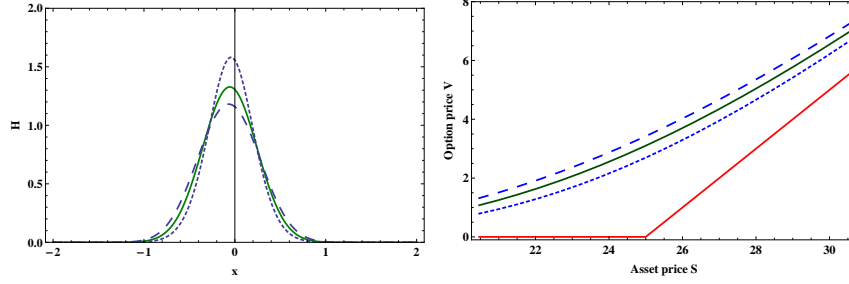


Fig. 1 A comparison of Bid and Ask option prices computed by means of the RAPM model for a call option in time $T - t = 1$. Left (right) figure presents the results before (after) the backward transformation. The blue dashed (fine-dashed) curve indicates the Ask (Bid) price of a call option. Green curve represents the option prices computed by the linear Black-Scholes model and the red line is the payoff function. Parameters: $n = 80$, $h = 0.025$, $m = 160$, $k = 0.00625$, $\tau^* = 0.00391$, $\hat{\sigma} = 0.30$, $\mu = \pm 0.2$, $r = 0.011$, $q = 0.0$, $X = 25$.

in the table 3. Since the total error is influenced not only by the discretization error, but also by the error related to the regularization and backward transformation, the Crank-Nicolson method exhibits EOC slightly below the second order. Finally, in figure 1 we present the numerical solution of the RAPM model for a call option using parameter τ^* obtained by the above described strategy but considering nonzero μ . Such an experiment is of particular interest also for practical applications.

Table 3 Outputs obtained by solving numerically Gamma equation (12) ($\tau_0 = 0$, $k = h/4$) using the Crank-Nicolson type scheme and using formula (13) for backward transformation.

n	h	τ^*	$\ e_n^m\ _{L_2}$	$EOC_{k \sim h}$	CPU Gamma	CPU Trans-form	CPU Total
5	0.4	0.46765	4.0644	-	0.047	0.011	0.058
10	0.2	0.14602	1.4586	1.4784	0.141	0.016	0.157
20	0.1	0.04371	0.4617	1.6595	0.624	0.047	0.671
40	0.05	0.01269	0.1379	1.7432	2.372	0.187	2.559
80	0.025	0.00361	0.0399	1.787	9.173	0.843	10.016
160	0.0125	0.00101	0.0113	1.816	41.091	3.323	44.414
320	0.00625	0.00028	0.0031	1.8270	150.525	12.87	163.396

Experiment with an exact (Barenblatt) solution. The goal of the *third experiment* was to investigate the accuracy of the proposed Crank-Nicolson type scheme using exact solution of the following (porous-medium type) equation:

$$\partial_t v = \partial_x^2 (v^\omega), \quad x \in R, \quad t > 0, \quad \omega > 1 \quad (14)$$

which is a special case of the Gamma equation (6). The exact solution has the form $v(x, t) = \frac{1}{\omega(t)} \max \left[0, 1 - \left(\frac{x}{\omega(t)} \right)^2 \right]^{\frac{1}{\omega-1}}$, where $\lambda(t) = \left[\frac{2\omega(\omega+1)}{\omega-1} (t+1) \right]^{\frac{1}{\omega+1}}$ represents a sharp interface of the solution's finite support. EOC of the Crank-Nicolson type scheme in L_1 -norm, which is used due to the singularity in the exact solution, is equal to 2, see table 4.

Table 4 Numerical approximation of the Barenblatt exact solution using Crank-Nicolson type scheme.

n	h	$\ e_n^m\ _{L_1}$	CPU	$EOC_{k \sim h}$
25	0.1	0.000629	0.312	-
50	0.05	0.000173	1.139	1.8584
100	0.025	0.000048	4.258	1.8543
200	0.0125	0.000012	17.036	1.9161
400	0.00625	$3.31 \cdot 10^{-6}$	67.798	1.9399
800	0.003125	$8.52 \cdot 10^{-7}$	250.475	1.9597
1600	0.0015625	$2.16 \cdot 10^{-7}$	881.905	1.97824

4 Conclusions

In this paper we proposed a new nonlinear second order Crank-Nicolson type numerical scheme based on the finite volume method. Our main goal was to provide an efficient and precise numerical solution to nonlinear PDEs arising in financial mathematics. Various experiments have shown such properties of the new scheme.

Acknowledgement. This work was supported by grants APVV-0351-07 and VEGA 1/0733/10.

References

1. Avellaneda, M., Levy, A., and Paras, A.: Pricing and hedging derivative securities in markets with uncertain volatilities. *Applied Mathematical Finance* 2, 73-88 (1995)
2. Balažovjeh M., Mikula K.: A Higher Order Scheme for the Curve Shortening Flow of Plane Curves. *Proceedings of ALGORITMY, STU Bratislava*, 165–175 (2009)
3. Barles, G., and Soner, H. M.: Option pricing with transaction costs and a nonlinear Black-Scholes equation. *Finance Stoch.* 2, 4 369-397 (1998)
4. Black, F., and Scholes, M.: The pricing of options and corporate liabilities. *The Journal of Political Economy* 81, 637-654 (1973)
5. Frey, R.: Market illiquidity as a source of model risk in dynamic hedging in model risk. In *RISK Publications*. R. Gibson Ed., London, (2000)
6. Jandačka, M., Ševčovič, D.: On the risk-adjusted pricing-methodology-based valuation of vanilla options and explanation of the volatility smile. *J. Appl. Math.* 3, 235-258 (2005)
7. Kratka, M.: No mystery behind the smile. *Risk* 9, 67-71 (1998)
8. Kwok, Y. K.: *Mathematical models of financial derivatives*. Springer-Verlag Singapore, Singapore (1998)
9. Leland, H. E.: Option pricing and replication with transaction costs. *Journal of Finance* 40, 1283-1301 (1985)
10. Merton, R.: Theory of rational option pricing. *The Bell Journal of Economics and Management Science*, 141-183 (1973)
11. Mimura, M., Tomoeda, K.: Numerical approximations to interface curves for a porous media equation. *Hiroshima Math. J.* 13, Hiroshima University, 273–294 (1983)
12. Schönbucher, P. J., and Wilmott, P.: *SIAM J. Appl. Math.* 61, 1, 232-272 (2000)
13. Ševčovič, D., Stehlíkova, B., Mikula, M.: *Analytical and numerical methods for pricing financial derivatives*. Nova Science Publishers, Hauppauge NY (2011)
14. Wilmott, P., Dewynne, J., Howison, S.: *Option Pricing: Mathematical Models and Computation*. Oxford Financial Press, Oxford (1993)